METABOLIC ENGINEERING 1, 35–48 (1999)
ARTICLE NO. MT980106

# Response of the Central Metabolism in *Corynebacterium glutamicum* to the use of an NADH-Dependent Glutamate Dehydrogenase

Achim Marx, Bernhard J. Eikmanns, Hermann Sahm, Albert A. de Graaf, and Lothar Eggeling

*Institut für Biotechnologie, Forschungszentrum Jülich GmbH, D-52425 Jülich, Germany*

E-mail: l.eggeling@fz-juelich.de

Received February 23, 1998; revised June 15, 1998; accepted July 2, 1998

**The extensive use of $^{13}C$ enrichments in precursor metabolites for flux quantification does not rely on NADPH stoichiometries and can therefore be used to quantify reducing power fluxes. As an application of this concept, the NADPH fluxes were quantified in an L-lysine producer of *Corynebacterium glutamicum* grown into metabolic and isotopic steady state with [1-$^{13}C$]glucose. In this case, where the organism's NADPH-dependent glutamate dehydrogenase consumes reducing power, the NADPH flux generated is 210% (molar flux relative to glucose uptake rate) with its major part (72% of the total) generated via the pentose phosphate pathway activity. An isogenic strain in which the glutamate dehydrogenase of *C. glutamicum* was replaced by the NADH-dependent glutamate dehydrogenase of *Peptostreptococcus asaccharolyticus* was made and the metabolite fluxes were again estimated. The major response to this local perturbation is a drastically reduced NADPH generation of only 139%. Most of the NADPH (62% of the total) is now generated via the tricarboxylic acid cycle activity. This shows the extraordinary flexibility of the central metabolism and provides a picture of the global regulatory properties of the central metabolism. Furthermore, a detailed analysis of the fluxes and exchange fluxes within the anaplerotic reactions is given. It is hypothesized that these reactions might also serve to balance the total reducing power budget as well as the energy budget within the cell.** © 1999 Academic Press

***Key Words:*** **reducing power supply; lysine production; anaplerotic reactions; pentose phosphate pathway; flux quantifications; isotope studies.**

## 1. INTRODUCTION

The fueling reactions within the central metabolism serve to provide energy as well as precursor metabolites for the cell. This dual function could be of particular importance when metabolite overproduction is attempted, since removal of precursors and an altered energy budget require a readjustment of the fluxes in this part of the metabolism. Metabolic engineering tries to make specific predictions of where increased activities could lead to a product increase. Such predictions are corroborated for reactions within assembling pathways, where allosterically controlled enzymes and branching points are major targets for obtaining flux increase (Eggeling *et al.*, 1996). Examples are the successful construction of amino-acid-producing-bacteria such as *Corynebacterium glutamicum* (Eggeling *et al.*, 1997a) or *Escherichia coli* (Eggeling and Sahm, 1998). Moreover, as a further target for improving metabolite production, a specific product exporter has recently been identified (Vrljic *et al.*, 1996). This completes the identification of the cellular control steps for converting precursors of the central metabolism into the desired extracellular product. However, in contrast to the assembling pathways and the transport process, the targets in the central metabolism to be engineered are less well defined. This is due to (i) the many branching points and cyclic and parallel reactions, (ii) the not easily accessible tools for quantifying the *in vivo* fluxes, (iii) the fact that enzyme activities in the network may be overlooked, and last but not least (iv) the very flexible responses of the living cell. Therefore, it is still a very ambitious goal to predict targets for flux increase in this part of the metabolism. A recent success in engineering the flux of glucose-derived carbons toward aromatic amino acid formation was based on more qualitative physiological knowledge (Flores *et al.*, 1996) and the successful application in producer strains has not yet been documented (Barry, 1996).

Of course, one aspect of metabolic engineering is a quantification of all fluxes. We have developed a comprehensive methodology distinguished by (i) the analysis of fluxes in the steady state, (ii) the intensive use of carbon atom quantification, made possible through [1-$^{13}C$]glucose and NMR spectroscopy, and (iii) metabolite balances (Marx *et al.*, 1996). This approach is completed by (iv) sophisticated mathematical tools also allowing the estimation of reverse fluxes and statistical parameters (Wiechert *et al.*, 1997). In particular, the high resolution obtained by such analyses in formulating new questions, whose answers could then in the future be utilized for metabolic engineering. This is the special benefit of intracellular flux analysis. In our previous



1096-7176/99 $30.00
Copyright © 1999 by Academic Press
All rights of reproduction in any form reserved.

investigations, we simply quantified the fluxes in isogenic *C. glutamicum* strains in a cause–effect study, where the central metabolism itself was not engineered, but only the final biosynthesis sequence or the export (Marx *et al.*, 1996, 1997). This served to probe the flexibility of the fueling reactions in response to different carbon burdens.

However, in most flux analyses no access to the reducing power budget has been possible to date. In contrast, NADP(H) stoichiometries are generally used as additional constraints to make solutions for carbon fluxes possible at all. In contrast, our approach, depending heavily on information on the fate of carbon atoms, does not require these constraints. Access to the reducing power budget is thus possible, since some carbon fluxes, e.g., through the glucose-6-phosphate dehydrogenase or the isocitrate dehydrogenase reaction, are inevitably linked to the NADPH flux. Therefore, carbon fluxes can be used to derive NADPH stoichiometries. We have already performed such calculations in previous work to a certain extent (Sonntag *et al.*, 1995). In the present paper, we describe our direct intervention in the NADPH budget to once again quantify the flexibility within the fueling reactions in a cause–effect study. Whereas we previously quantified the response of the central metabolism due to different carbon flux burdens (Marx *et al.*, 1997), this time we focus on the response of the central metabolism to different reducing power demands.

## MATERIALS AND METHODS

### *Genetic Engineering*

The *Peptostreptococcus asaccharolyticus* glutamate dehydrogenase gene was cloned according to the published sequence (Snedecor *et al.*, 1991) by use of the polymerase chain reaction and the primers 5′-ATGGATCCCCGAGT GAGAAATCACGGTG-3′ and 5′-CTGAGCTCAGCTGA TTATATGAGTTT-3′. The 1.4-kb product obtained was digested with *Bam*HI and *Sac*I and ligated with the shuttle vector pEKEx2 treated identically (Eikmanns *et al.*, 1991). Transformation of *E. coli* DH5α yielded kanamycin-resistant clones which were confirmed by restriction analyses to contain pEKExpgdh of 9.7 kb (Fig. 1). With this vector the specific glutamate dehydrogenase activity (NADH as substrate, *E. coli* as host) was increased from 0.05 to 1.1, and, after isopropyl-β-D-thiogalactoside addition, to 5.4 μmol/min and mg protein.

For construction of the gene deletion vector pK19*mobsacBΔgdh*, part of the *gdh* gene was isolated as a 1.25-kb *Sph*I fragment (Börmann *et al.*, 1992) and ligated with pUC18. A *Bgl*II and *Eco*RV site within *gdh* was used to remove a 611-bp internal fragment to result in pUC18*Δgdh*. The *Sph*I fragment, now only 0.6 kb in size, was reisolated

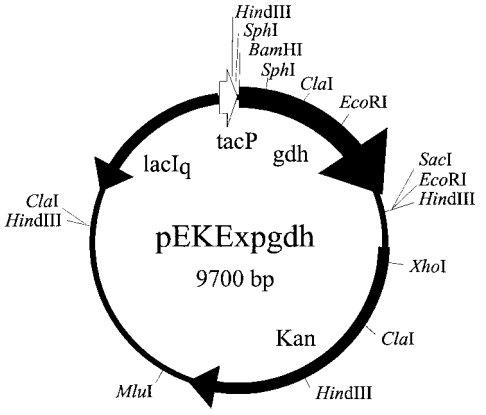


**FIG. 1.** The expression vector pEKEXpgdh to express the NAD-dependent *Peptostreptococcus asaccharolyticus* glutamate dehydrogenase gene *gdh* in *C. glutamicum*. Abreviations: *Kan*, kanamycine resistance; *lacI*$^q$, the constitutively expressed repressor of the *lac* operon; *tacP*, *Tac* promotor.

and ligated with the vector pK19*mobsacB*, which had been previously cleaved with *Sph*I and treated with alkaline phosphatase. The resulting vector pK19*mobsacBΔgdh* was introduced into the mobilizing donor strain *E. coli* S17-1 (Simon *et al.*, 1983), and matings were performed with *C. glutamicum* MH20-22B (Schrumpf *et al.*, 1992) according to Schäfer *et al.* (1990). The single transconjugant obtained was cultivated overnight in liquid LBG for proliferation, and then dilutions were spread on LBG containing 10% sucrose (Schäfer *et al.*, 1994) to select for clones where the second recombination had taken place. One hundred Suc$^r$ clones were assayed for their kanamycin phenotype, and eventually 15 Suc$^r$ Kan$^s$ clones were subjected to glutamate dehydrogenase activity determinations.

The enzymes necessary for *in vitro* recombinations were obtained from Boehringer (Mannheim, Germany) and used as recommended. Plasmids were isolated as described (Schwarzer and Pühler, 1990). *E. coli* was transformed after pretreatment with $CaCl_2$/$RbCl_2$ and *C. glutamicum* by electroporation (Liebl *et al.*, 1989).

### *Continuous Culture*

The strains (homologous mutant strain *C. glutamicum* MH20-22B*Δgdh* pEK1.9*gdh*-1 and heterologous mutant strain *C. glutamicum* MH20-22B*Δgdh* pEKExpgdh) were grown in continuous culture as described elsewhere (Marx *et al.*, 1996). The medium was identical to that previously used with 43 mM glucose and 1.4 mM L-leucine, except that the ammonium sulfate concentration was 600 mM, and isopropyl-β-D-thiogalactoside (IPTG) (0.5 mM) and methionine S-sulfoximine (14.8 mM) were present. After inoculation and consumption of glucose, the medium together with [1-$^{13}$C]glucose was fed continuously at a rate of 0.082 h$^{-1}$.

**TABLE I**

**Extracellular Fluxes in Two L-Lysine-Producing Strains of *C. glutamicum* Differing Only in the Possession of an NAD or NADPH-Dependent Glutamate Dehydrogenase**

| | Glutamate dehydrogenase | |
|---|---|---|
| Carbon[a] | *gdh*(NAD) | *gdh*(NADP) |
| Glucose | 100 | 100 |
| Biomass | 33 | 28 |
| Product | 18 | 32 |
| $CO_2$ | 45 | 39 |
| Sum | 96 | 99 |
| $Y_{X/S}$ ($g_X \cdot g_S^{-1}$) | 0.33 | 0.28 |
| $Y_{P/S}$ ($mol_P \cdot mol_S^{-1}$) | 0.18 | 0.32 |
| $q_S$ ($nmol_S \cdot min^{-1} \cdot mg_{DW}^{-1}$) | 23.0 | 26.9 |

*Note.* Abbreviations: *gdh*(NAD) are the data for the strain with the NAD-dependent glutamate dehydrogenase of *Peptostreptococcus asaccharolyticus*, *gdh*(NADP) those for the strain with the NAD-dependent enzyme. $Y_{X/S}$ ($Y_{P/S}$) is the yield of conversion of the substrate glucose (S) to biomass (X), and product (P), respectively. $q_S$ is the specific substrate uptake rate.

[a] Expressed as percentage of consumed glucose carbon.

$CO_2$ evolution as well as the dissolved oxygen concentration of the culture, was recorded on-line. In the steady state, glucose was entirely consumed. Samples of the cultures were collected to estimate lysine, growth, NADH- and NADPH-dependent glutamate dehydrogenase activities, and glutamine–oxoglutarate aminotransferase activity. In addition, in the steady state the $^{13}CO_2$ content of the effluent gas was quantitated by nondispersive infrared spectroscopy. From the analyses, the carbon balances of the cultures were derived which are given in Table 1 as percentages of flux relative to the glucose input rate.

### *Enzyme Determinations*

Cells were harvested from the chemostat or exponentially growing cultures. They were washed with 0.9% NaCl, resuspended in the respective assay buffer, and disrupted by sonification. The cell debris was removed by centrifugation, and the resulting crude extract was used directly for glutamate dehydrogenase activity determinations. For determination of the glutamine–oxoglutarate aminotransferase activity (GOGAT), crude extract was gel-filtrated (PD-10 columns, Pharmacia) to remove ammonium salts, using as eluent buffer 0.1 M potassium phosphate (pH 7.5), 1.44 mM cysteine, 0.5 mM EDTA.

The glutamate dehydrogenase activity was assayed by following the oxoglutarate-dependent decrease in the extinction at 340 nm. The assay contained, in 1 ml, 100 $\mu$mol Tris/HCl buffer (pH 8.0), 0.25 $\mu$mol NADPH (or NADH, respectively), 20 $\mu$mol $NH_4Cl$, and 10 $\mu$mol 2-oxoglutarate. The GOGAT activity was assayed in a system containing, in 1 ml, 100 $\mu$mol Tris/HCl buffer (pH 7.6), 0.1 $\mu$mol dithiothreitol, 0.25 $\mu$mol NADPH, 10 $\mu$mol 2-oxoglutarate, and 10 $\mu$mol glutamine. The protein concentration in the extracts was determined by the biuret method using bovine serum albumin as standard.

### *Determination of Fractional Enrichments in Carbon Atoms*

High-resolution $^1H$ NMR spectra were obtained on an AMX-400 WB spectrometer (Bruker, Karlsruhe, Germany) operating at 400.13 MHz and equipped with a multichannel interface and a 5-mm inverse GRASP probe head. For the determination of $^{13}C$ enrichments in the protonated carbon atoms, as well as in the nonprotonated carbon atoms, $^1H$ NMR difference spectroscopy with and without GARP-1 composite pulse $^{13}C$ decoupling was used. The $^{13}C$ enrichments of protonated carbons were calculated as the ratio of the $^{13}C$ satellite signal area in the difference spectrum to the total integral of each proton in the GARP-1 decoupled spectrum. For the determination of $^{13}C$ enrichments in the nonprotonated carbons, spin-echo NMR spectroscopy was applied (Wendisch *et al.*, 1997). Typical settings of the inversion pulse sequence were 15-s relaxation delay, 2-s $H_2O$ presaturation pulse; 9 $\mu$s 90° transmitter pulse; and 256-$\mu$s sine-shaped spoiler delay, with a selective 18-$\mu$s 180° transmitter pulse, and a 180° decoupler inversion pulse adjusted sample-specific. GARP-1 decoupling was optionally used.

The $^{12}CO_2$ concentration in the exhaust gas was measured on-line by non-dispersive infrared spectroscopy (URAS 10E, Hartmann & Braun, Frankfurt, Germany). The $^{13}CO_2$ concentration was quantified off-line by infrared spectroscopy with appropriate standards and settings (COI, Fischer Analysen GmbH, Leipzig, Germany).

### *Flux Determinations*

The precursor demand for cell mass formation is as described (Marx *et al.*, 1996), as well as the biochemical model used (Marx *et al.*, 1997). The mathematical treatment has been described in detail by Wiechert *et al.* (1997) using matrix notations of the carbon-labeling balance equations. The program NMRFlux was used (Wiechert and de Graaf, 1997) to convert the biochemical equations and the equations of carbon atom transitions into the corresponding flux equations. Similarly, the experimentally determined fluxes and enrichments were incorporated. Using a sophisticated parameter-fitting algorithm (Wiechert *et al.*, 1997), which is based on the Levenberg–Marquard algorithm, a nonlinear least-squares analysis with mutiple initializations was performed to determine the global minimum.

## RESULTS

### *Engineering of Strains*

The rationale of the NADPH flexibility study in *C. glutamicum* was to use an NADH-consuming glutamate dehydrogenase instead of the original NADPH-dependent enzyme of the organism (Oshima *et al.*, 1964; Börmann *et al.*, 1992). Such an NADH-consuming enzyme is present in *P. asaccharolyticus*, where it serves catabolic purposes (Snedecor *et al.*, 1991). Of course, when dictated by the equilibrium constant, the enzyme also catalyzes the formation of glutamate. Based on the published sequence and using the polymerase chain reaction, we amplified the *P. asaccharolyticus* glutamate dehydrogenase gene from genomic DNA. A *Bam*HI site was introduced 39 bp in front of the gene and a *Sac*I site 163 bp downstream of it. This served to clone the amplified fragment into the corresponding sites of the expression vector pEKEx2 (Eikmanns *et al.*, 1991) to yield pEKExpgdh. With this vector, NAD-dependent and IPTG-inducible glutamate dehydrogenase activity was obtained in *C. glutamicum* (see below).

To delete the original NADPH-dependent enzyme from the *C. glutamicum* chromosome, the mobilizable but non-replicative vector pK19*mobsacB*Δ*gdh* was constructed (see Materials and Methods). It carries the homologous *C. glutamicum* gene, from which an internal fragment had been deleted. It was introduced into the lysine producer *C. glutamicum* MH20-22B by intergeneric mating. This lysine producer was chosen because (i) the NADPH demand for lysine production is high, (ii) the strain is very well characterized (Schrumpf *et al.*, 1992), and (iii) we have already established several detailed flux quantifications for this high-level producer (Marx *et al.*, 1996, 1997). After mating, one transconjugant (resistant for kanamycin) was obtained with the vector integrated in the chromosomal *gdh* due to homologous recombination. This clone was subjected to a second round of positive selection (resistance for sucrose) to result in clones which had lost the vector. Fifteen of the numerous clones obtained were assayed for glutamate dehydrogenase activity, and three of them were identified as having no enzyme activity due to the appropriate location of the second recombination. The loss of the chromosomal fragment in the constructed strain *C. glutamicum* MH20-22BΔ*gdh* was confirmed in a Southern blot (not shown). This strain was transformed with plasmid pEKExpgdh, encoding the heterologous *P. asaccharolyticus* enzyme. As the control, the deletion strain was transformed with pEK1.9*gdh*-1, encoding the homologous *C. glutamicum* enzyme (Börmann *et al.*, 1992). In the following the strains will be referred to as the heterologous mutant and the homologous mutant, respectively.

### *Gene Expressions*

To verify expression of the glutamate dehydrogenase genes, enzyme activity determinations were performed. In the strain MH20-22BΔ*gdh* with deleted dehydrogenase, no enzyme activity was detected (not shown). In the heterologous mutant with the *P. asaccharolyticus* gene, the NADH-dependent enzyme was synthesized (without IPTG addition) to yield a high specific dehydrogenase activity of 1.80 $\mu$mol/min/mg protein. In addition to the dehydrogenase activity residual glutamine–oxoglutarate aminotransferase activity was detectable in this heterologous mutant (activity of 0.033 $\mu$mol/min/mg protein); it was almost zero in the homologous mutant. Since this activity, together with the glutamine synthetase, could contribute to NADPH-dependent glutamate synthesis, the inhibitor methionine *S*-sulfoximine was used (Weisbrod and Meister, 1973). *In vivo* this inhibitor specifically prevents glutamate synthesis via the transferase/glutamine synthetase system, since growth of *C. glutamicum* with inactivated *gdh* is abolished at a concentration of 10 mM, whereas growth of the wild type is not (M. Tesch, personal communication). Consequently, both the heterologous mutant and the homologous mutant were grown in the continuous cultures in the presence of 15 mM methionine *S*-sulfoximine. As verified in extracts of cells taken from the cultures during establishment of the steady state, the dehydrogenase activities in both cultures were already comparable after 3 and 4 volume changes. In the steady state, a specific activity of 5.08 $\mu$mol/min/mg protein was determined for the NAD-dependent enzyme of the heterologous mutant, and a specific activity of 6.97 $\mu$mol/min/mg protein for the NADP-dependent enzyme of the homologous mutant was determined.

### *NMR Quantifications*

Continuous cultures of the mutants were supplied with 99% enriched [1-$^{13}$C]glucose. In the steady state all glucose was consumed. Making use of the fact that in the metabolic and isotopic steady state the enrichments in the precursors within the metabolic network are identical to those in the precursors stored as building blocks in the cell material, we hydrolyzed the total cell material and isolated the building blocks on a preparative scale to allow enrichment determinations. In total, the fractional enrichments in carbon in nine amino acids, in glucosamine, and in the sugar moiety of guanosine were quantified by $^{1}$H-detected NMR spectroscopy, including spin-echo NMR for non-protonated carbons of amino acids (Tables 2 and 3).

As a technique generally applicable to quantifying the enrichment in $CO_2$, a method for estimating the enrichment

**TABLE II**

**Measured $^{13}C$ Enrichments in Cell Constituents Isolated from the Heterologous Mutant, *gdh*(NAD)**

| Metabolite | $^{13}C$ enrichment (%) in carbon | | | | | |
|---|---|---|---|---|---|---|
| | C-1 | C-2 | C-3 | C-4 | C-5 | C-6 |
| Gly | $3.2 \pm 0.3$ | $2.2 \pm 0.3$ | | | | |
| Ala | $4.3 \pm 1.0$ | $4.5 \pm 1.0$ | $37.0 \pm 0.8$ | | | |
| Glx | $18.6 \pm 0.6$ | $30.1 \pm 0.6$ | $18.3 \pm 0.2$ | $37.5 \pm 0.4$ | $3.6 \pm 1.0$ | |
| Arg | n.d. | $30.7 \pm 1.0$ | $18.4 \pm 1.0$ | $35.1 \pm 1.0$ | $2.9 \pm 1.0$ | $16.4 \pm 0.5$ |
| Thr | $12.6 \pm 0.8$ | n.d. | n.d. | $16.2 \pm 1.5$ | | |
| Asx | n.d. | $18.1 \pm 1.0$ | $30.7 \pm 1.5$ | n.d. | | |
| Phe[a] | n.d. | n.d. | $34.3 \pm 2.5$ | n.d. | $20.5 \pm 2.5$ | $1.1 \pm 1.0$ |
| Val[b] | n.d. | $4.8 \pm 1.0$ | n.d. | $37.4 \pm 1.5$ | | |
| Lys | n.d. | $13.2 \pm 0.6$ | $30.2 \pm 1.0$ | $15.5 \pm 1.0$ | n.d. | $7.6 \pm 0.4$ |
| Guanosine | $24.5 \pm 0.8$ | n.d. | n.d. | n.d. | $25.1 \pm 1.0$ | |
| Glucosamine | $78.0 \pm 4.0$ | n.d. | n.d. | n.d. | n.d. | n.d. |
| $CO_2$ | $16.5 \pm 0.5$ | | | | | |

*Note.* n.d., not determined.
[a] The mean value for C-5 is derived from C-5 plus C-9. The enrichment in C-7 and C-8 is $1.1 \pm 1.0$%.
[b] The mean value for C-4 is derived from C-4 plus C-4′.

in C-6 of arginine was developed because the C-6 enrichment stems exclusively from $CO_2$ incorporated via carbamoylphosphate synthase activity. In a series of experiments, the spin-echo delay (TE) was varied to quantify the amplitudes of the $^{13}C$ satellites in the difference spectra obtained. A cosine dependency of the amplitudes of the difference spectra on TE is observed due to the evolution of the long-range *J* HCNC during the spin-echo delay (Fig. 2). According to the difference signal of 30.7% for the heterologous mutant, a spin-echo delay of 142 ms and calibration result in a fractional enrichment of $16.5 \pm 0.5$%. This is in excellent agreement with the enrichment in $CO_2$ as determined by nondispersive infrared spectroscopy (Table 2). It shows that in the culture the intracellular $CO_2$ is in equilibrium with the extracellular $CO_2$. Access to the fructose 6-phosphate enrichments was made possible by the quantifications in glucosamine. Together with the available enrichments in e4p and p5p, this further improves the flux

**TABLE III**

**Measured $^{13}C$ Enrichments in Cell Constituents Isolated from the Homologous Mutant, *gdh*(NADP)**

| Metabolite | $^{13}C$ enrichment (%) in carbon | | | | | |
|---|---|---|---|---|---|---|
| | C-1 | C-2 | C-3 | C-4 | C-5 | C-6 |
| Gly | $2.0 \pm 0.2$ | $1.7 \pm 0.3$ | | | | |
| Ser | n.d. | n.d. | $23.0 \pm 2.0$ | | | |
| Ala | $2.0 \pm 0.5$ | $2.2 \pm 1.0$ | $25.7 \pm 0.7$ | | | |
| Glx | $15.7 \pm 0.6$ | $21.1 \pm 0.3$ | $11.6 \pm 0.3$ | $25.8 \pm 0.7$ | $2.2 \pm 1.0$ | |
| Arg | n.d. | $20.5 \pm 0.5$ | $11.6 \pm 1.0$ | $23.9 \pm 1.0$ | $1.9 \pm 1.0$ | $21.3 \pm 0.4$ |
| Thr | $8.0 \pm 0.5$ | $12.7 \pm 1.0$ | $20.4 \pm 1.7$ | $15.3 \pm 1.0$ | | |
| Phe[a] | n.d. | $1.1 \pm 1.0$ | $25.5 \pm 1.0$ | n.d. | $12.8 \pm 2.0$ | $1.1 \pm 1.0$ |
| Val[b] | n.d. | $2.6 \pm 1.0$ | $2.6 \pm 1.0$ | $26.0 \pm 2.5$[b] | | |
| Lys | n.d. | $8.2 \pm 0.4$ | $22.2 \pm 1.0$ | $14.8 \pm 1.0$ | n.d. | $3.7 \pm 0.4$ |
| Guanosine | $7.5 \pm 0.4$ | $2.9 \pm 1.3$ | $1.1 \pm 1.0$ | $1.1 \pm 1.0$ | $16.4 \pm 0.6$ | |
| Glucosamine | $62.3 \pm 2.5$ | n.d. | n.d. | n.d. | n.d. | n.d. |
| $CO_2$ | $22.4 \pm 0.5$ | | | | | |

[a] The mean value for C-5 is derived from C-5 plus C-9. The enrichment in C-7 and C-8 is $1.1 \pm 1.0$%.
[b] The mean value for C-4 is derived from C-4 plus C-4′.

**TABLE IV**

**$^{13}$C Enrichments in Precursor Metabolites of the Heterologous Mutant as Derived from the Experimentally Determined Enrichments (Standard Characters) and as Predicted by the Solution of the Mathematical Model for Flux Quantification (in Italics)**

| Metabolite | $^{13}$C enrichment (%) in carbon | | | | | |
|---|---|---|---|---|---|---|
| | C-1 | C-2 | C-3 | C-4 | C-5 | C-6 |
| f6p | 78.0 ± 4.0 | n.d. | n.d. | n.d. | n.d. | n.d. |
| *f6p* | *80.0* | *1.4* | *4.6* | *1.6* | *1.3* | *9.6* |
| p5p | 24.5 ± 0.8 | n.d. | n.d. | n.d. | 25.1 ± 1.0 | |
| *p5p* | *24.4* | *2.3* | *2.4* | *1.6* | *24.9* | |
| e4p | 1.1 ± 1.0 | 1.1 ± 1.0 | 1.1 ± 1.0 | 20.5 ± 2.5 | | |
| *e4p* | *2.9* | *2.2* | *1.5* | *20.9* | | |
| gap | 3.2 ± 0.3 | 2.2 ± 0.3 | n.d. | | | |
| *gap* | *3.1* | *1.9* | *37.9* | | | |
| pyr | 4.3 ± 1.0 | 4.6 ± 1.0 | 37.2 ± 1.5 | | | |
| *pyr* | *4.0* | *3.6* | *37.2* | | | |
| akg | 18.6 ± 0.6 | 30.1 ± 0.6 | 18.3 ± 0.2 | 37.5 ± 0.4 | 3.6 ± 1.0 | |
| *akg* | *16.3* | *30.6* | *18.2* | *37.2* | *3.7* | |
| oaa | 12.6 ± 0.8 | 18.1 ± 1.0 | 30.7 ± 1.5 | 16.2 ± 1.5 | | |
| *oaa* | *11.7* | *18.2* | *30.6* | *16.3* | | |
| lys | n.d. | 13.2 ± 0.6 | 30.2 ± 1.0 | 15.5 ± 1.0 | n.d. | 7.6 ± 0.4 |
| *lys* | *9.5* | *14.0* | *32.5* | *16.3* | *35.3* | *7.8* |
| $CO_2$ | 16.4 ± 0.5 | | | | | |
| *$CO_2$* | *16.4* | | | | | |

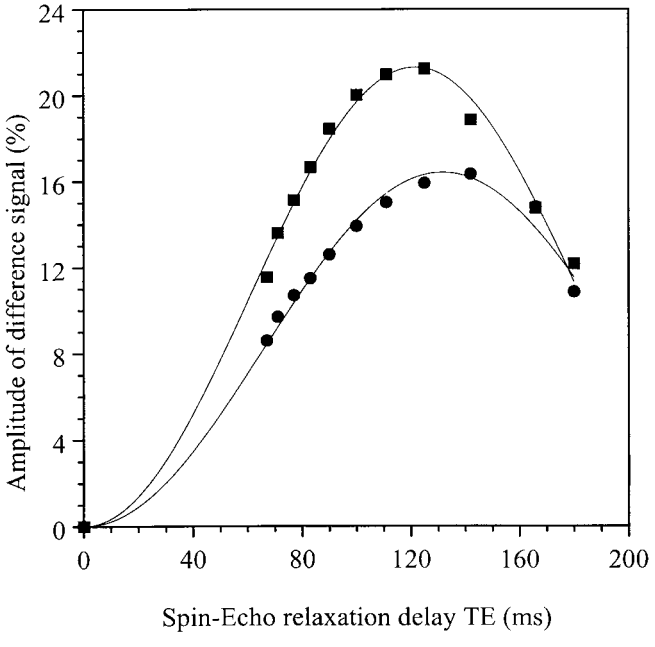


**FIG. 2.** Spin-echo difference signal amplitude of $^{13}$C-6 satellites of H-5 of arginine as a function of the spin-echo relaxation delay, from arginine isolated from the homologous mutant (■) and from the heterologous mutant (●) after growth on [1-$^{13}$C]-glucose.

determinations within the pentose phosphate pathway (PPP).

The fractional enrichments in the precursor metabolites of the heterologous mutant thus derived are given in Table 4. For those positions where several data were available (for instance, C-1 pyr derived from C-1 ala and C-1 val), a weighted mean value was used. Weighting was performed according to the measurement error. In a similar manner, the data for the precursor metabolites of the homologous mutant were derived and are given in Table 5.

### *Estimated Carbon Fluxes*

The current model used to estimate the carbon fluxes contains 14 fluxes removing or supplying metabolites from the network, with 11 of them being accumulating fluxes for biomass synthesis. Another 16 fluxes connect the 14 intracellular metabolite pools in the central metabolism (Marx *et al.*, 1997). For each experiment a detailed statistical analysis was carried out according to the procedures described by Wiechert *et al.* (1997). In particular, confidence regions and correlations were computed for the estimated fluxes (Table 6). The sums of squared deviations were 32.9 and 48.7 for the heterologous and the homologous mutant,

**TABLE V**

**$^{13}$C Enrichments in Precursor Metabolites of the Homologous Mutant as Derived from the Experimentally Determined Enrichments (Standard Characters) and as Predicted by the Solution of the Mathematical Model for Flux Quantification (in Italics)**

| Metabolite | $^{13}$C enrichment (%) in carbon | | | | | |
|---|---|---|---|---|---|---|
| | C-1 | C-2 | C-3 | C-4 | C-5 | C-6 |
| f6p | 62.3 ± 2.5 | n.d. | n.d. | n.d. | n.d. | n.d. |
| *f6p* | *61.7* | *1.5* | *2.5* | *1.4* | *1.3* | *8.5* |
| p5p | 7.5 ± 0.4 | 2.9 ± 1.3 | 1.1 ± 1.0 | 1.1 ± 1.0 | 16.4 ± 0.6 | |
| *p5p* | *7.6* | *2.1* | *1.6* | *1.5* | *16.4* | |
| e4p | 1.1 ± 1.0 | 1.1 ± 1.0 | 1.1 ± 1.0 | 12.8 ± 2.0 | | |
| *e4p* | *2.2* | *1.6* | *1.4* | *14.3* | | |
| gap | 2.0 ± 0.2 | 1.7 ± 0.3 | 23.0 ± 2.0 | | | |
| *gap* | *2.0* | *1.7* | *26.3* | | | |
| pyr | 2.0 ± 0.5 | 2.4 ± 1.0 | 25.7 ± 0.7 | | | |
| *pyr* | *2.0* | *1.9* | *26.2* | | | |
| akg | 15.7 ± 0.6 | 21.1 ± 0.3 | 11.6 ± 0.3 | 25.8 ± 0.7 | 2.2 ± 1.0 | |
| *akg* | *16.2* | *21.2* | *11.6* | *26.2* | *1.9* | |
| oaa | 8.0 ± 0.5 | 12.7 ± 1.0 | 20.4 ± 1.7 | 15.3 ± 1.0 | | |
| *oaa* | *7.9* | *11.6* | *21.2* | *16.2* | | |
| lys | n.d. | 8.2 ± 0.4 | 22.2 ± 1.0 | 14.8 ± 1.0 | n.d. | 3.7 ± 0.4 |
| *lys* | *6.4* | *9.1* | *22.5* | *16.2* | *24.9* | *4.4* |
| CO2 | 21.3 ± 0.4 | | | | | |
| *$CO_2$* | *23.2* | | | | | |

**TABLE VI**

**Statistical Analysis of Net or Exchange Fluxes in the Two Isogenic *C. glutamicum* Strains.**

| Flux | Reaction | Flux rate (%) of lower and upper boundary | | | |
|---|---|---|---|---|---|
| | | Homologous mutant | | Heterologous mutant | |
| $v_5$ | Glucose-6-P DH | 56.8 | 95.9 | 21.0 | 31.8 |
| $v_{15}$ | Isocitrate lyase | 0.0 | 0.0 | 0.0 | 5.6 |
| | Diaminopimelate DH | 11.3 | 17.3 | 6.2 | 9.2 |
| $v_1^{\leftrightarrow}$ | Glucose-6-P isomerase | 96.9 | ∞ | 0.0 | ∞ |
| $v_4^{\leftrightarrow}$ | Glyceraldehyde-3-P DH | 79.6 | ∞ | 36.8 | 132.5 |
| $v_8^{\leftrightarrow}$ | TK(x5p + e4p ↔ g3p + f6p) | 3.1 | 14.9 | 3.5 | 8.0 |
| $v_9^{\leftrightarrow}$ | TA | 0.0 | 9.4 | 6.4 | 20.3 |
| $v_{10}^{\leftrightarrow}$ | TK(x5p + ri5p ↔ s7p + g3p) | 54.4 | 74.7 | 30.0 | 46.6 |
| $v_{14}^{\leftrightarrow}$ | Fumarase | 22.4 | 41.2 | 16.2 | 50.2 |
| $v_{16}^{\leftrightarrow}$ | Anaplerotic exchange | 3.8 | 17.0 | 22.6 | 36.5 |

*Note*. The 90% confidence interval for the upper and lower boundary is given. The values are expressed as percentages relative to the glucose uptake flux (set to 100%). Abbreviations: DH dehydrogenase; TK, transketolase; TA, transaldolase. The fluxes are specified in detail in Marx *et al.* (1996).

respectively, showing good correspondence between measured and computed values.

The carbon fluxes estimated in the homologous mutant are shown in Fig. 3. The flux entering the PPP is as high as 76%. The excess carbon flux not required for the synthesis of polyolphosphates for biosynthetic purposes is over the nonoxidative transaldolase and transketolase reactions to f6p and gap, which thus rejoin the glycolysis. At the level of the gap 162 mol% is present out of the theoretical maximum of 200 mol%. This equals 81% of the maximum. Thus at the level of the gap, 19% of the carbon was used for biomass formation and carbon dioxide generation. In the heterologous mutant (Fig. 4), the flux entering the PPP is strongly reduced to 26%. This can be traced back to the enrichment in C-3 of pyr (compare Tables 4 and 5), since less C-1 of the substrate [1-$^{13}$C]glucose is removed from the network in this mutant. However, at the level of the gap, again 176 mol% is present. Thus the strong change in the oxidative part of the PPP has limited consequences for the gap availability, and for the fluxes towards pep and pyr. In both mutants the glyoxylic acid cycle carries no flux,

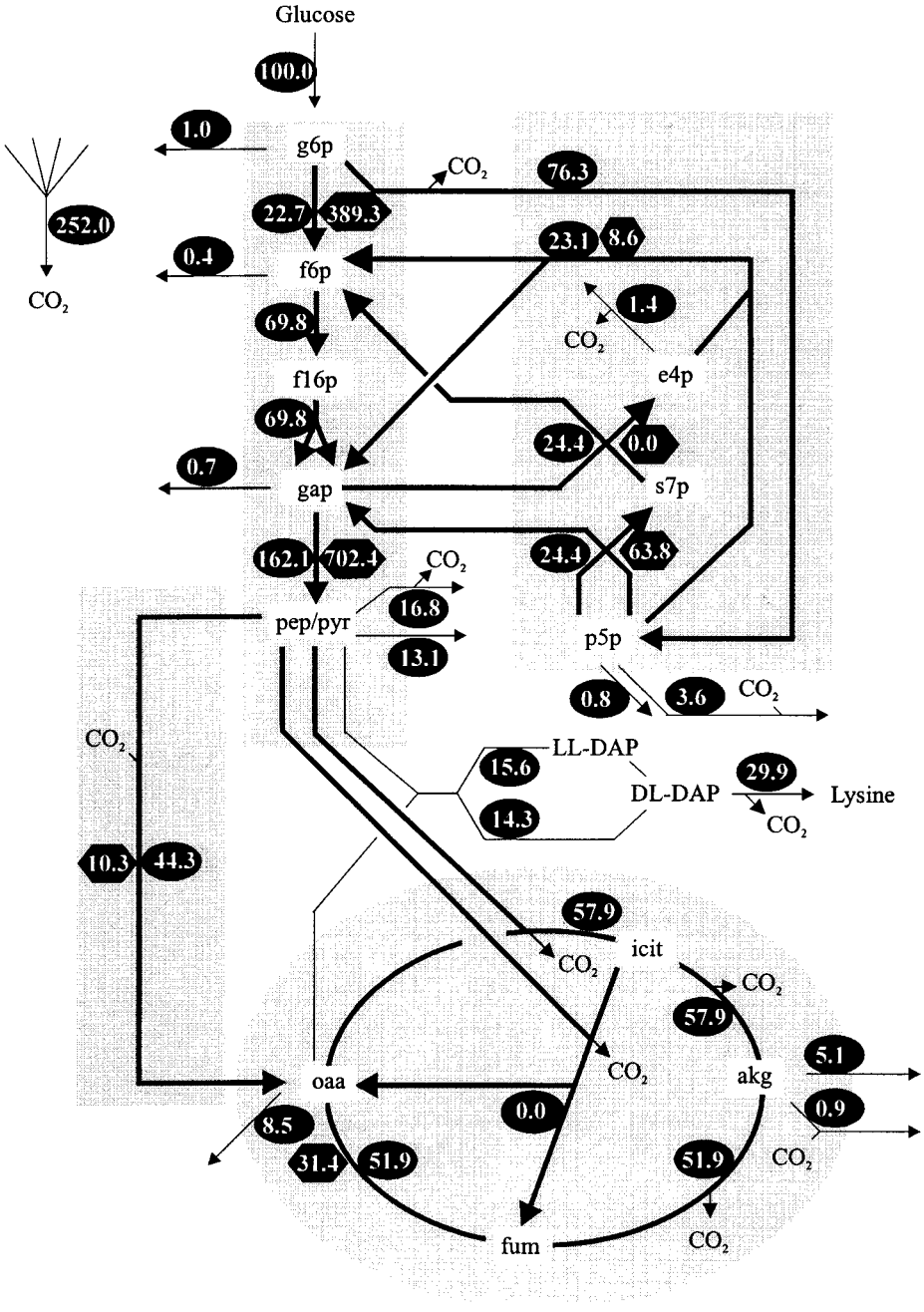


**FIG. 3.** *In vivo* flux distribution in the central metabolism for *C. glutamicum* MH20-22B using its NADP-dependent glutamate dehydrogenase (homologous mutant MH20-22B*Δgdh* pEK1.9*gdh*-1). Numbers in oval symbols near thick lines give the estimated net fluxes; those near the thin arrows give the measured fluxes required for biomass synthesis. Numbers in hexagons give the estimated additional exchange fluxes in reversible reactions. All fluxes are given as molar metabolite flux expressed as a percentage of the glucose uptake rate, which was 26.9 $\mu$mol/g dry. Abbreviations: g6p, glucose 6-phosphate; f16bp, fructose 1,6-bisphosphate; f6p, fructose 6-bisphosphate; gap, glyceraldehyde 3-phosphate; pep, phospho*enol*pyruvate; pyr, pyruvate; oaa, oxaloacetate; fum, fumarate; icit, isocitrate, akg, ketoglutarate; p5p, pentose 5-phosphate; s7p, sedoheptulose 7-phosphate; e4p, erythrose 4-phosphate; LL-DAP, LL-diaminopimelate; DL-DAP, DL-diaminopimelate.

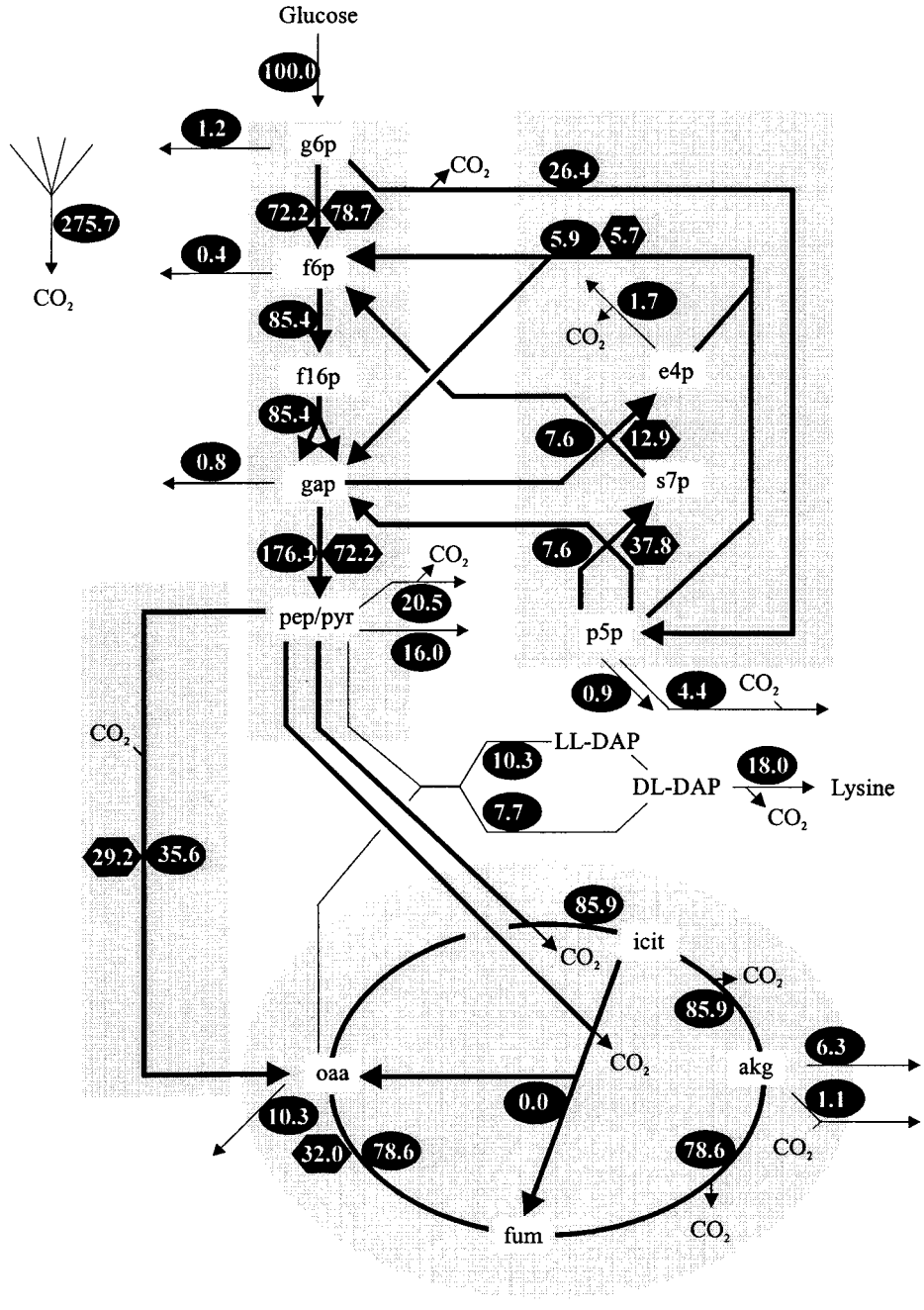


**FIG. 4.** *In vivo* flux distribution in the central metabolism for *C. glutamicum* MH20-22B using the NAD-dependent glutamate dehydrogenase of *P. asaccharolyticus* (heterologous mutant *C. glutamicum* MH20-22B*Δgdh* pEKEXpgdh). The glucose flux, set to 100% was 23.0 $\mu$mol/g dry. Description and abbreviations as in Fig. 3.

whereas the flux entering the tricaboxylic acid cycle (TCC) is significantly increased to 86 mol%, compared to the homologous mutant (58%). This could be due to an increased NADH demand in the heterologous mutant. In both mutants a high and comparable part of the lysine is synthesized via the dehydrogenase branch of the split pathway, which contributes 48% to total lysine synthesis in the homologous mutant and 43% in the heterologous mutant.

The exchange fluxes are shown in hexagons in Figs. 4 and 5, with their 90% confidence interval given in Table 6. For the heterologous mutant we estimated a large backflux

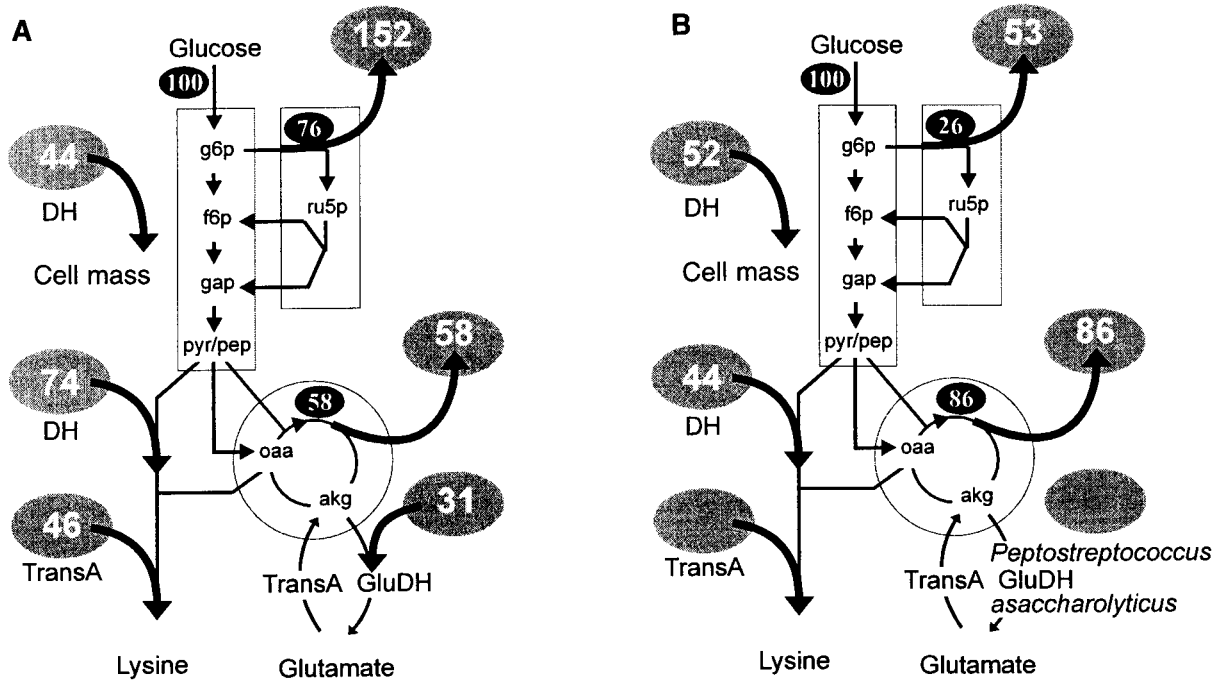


**FIG. 5.** The NADPH-generating and -consuming fluxes with NADPH-dependent glutamate dehydrogenase (A) and NADH-dependent glutamate dehydrogenase (B). The numbers in large ovals are the NADPH fluxes in mol% relative to the glucose uptake flux.

of 29.2 mol% (confidence interval 22.6–36.5) within the anaplerotic reactions. In the homologous mutant this value is only 10.3% (interval 3.8–17.0). This difference is reflected in the higher enrichment in C-2 of pyr in the heterologous mutant, which is due to the higher incorporation of oxaloacetate carbons via backflux into pyruvate. On the other hand, the enrichment in C-2 of oxaloacetate (oaa) decreases with high exchange flux (Fig. 6). In the computer-aided analysis all data are considered and contribute to the estimate of this exchange flux $v_{16}^{\leftrightarrows}$. Further high-exchange fluxes are present within the PPP, with the transketolase reaction ($p5p + p5p \leftrightarrow s7p + gap$) exceeding the net flux more than threefold. In the TCC a moderate backflux from oxaloacetate to fumarate was estimated.

### *The Estimated NADPH Fluxes*

For the NADPH-generating fluxes only three reactions are relevant. These are the glucose-6-phosphate dehydrogenase, gluconate-6-phosphate dehydrogenase and isocitrate dehydrogenase reactions, where the carbon flux is directly equivalent to molar NAPH generation (Fig. 5A). These generating fluxes add up in the homologous mutant to a molar flux of 210.5%. The malic enzyme was not considered because only a maximal value can be derived from the current flux analyses (see Discussion). To calculate the consuming fluxes we counted the required amounts of NADPH from known stoichiometries of the various biosynthetic reactions and the cell composition (Marx *et al.*, 1996). Approximately 15,500 $\mu$mol NADPH is necessary for the synthesis of 1 g dry weight. Of this amount about 50% is consumed by the glutamate dehydrogenase reaction, which functions mainly to deliver its amino group via transamination to cell mass synthesis (6350 $\mu$mol/g dry), and to a lesser extent to provide glutamate and glutamine for protein synthesis (800 $\mu$mol/g dry). Based on these stoichiometries the NADPH-consuming flux for α-ketoglutarate reduction is 31 mol%, and that directly required for reduction of cell material via dehydrogenases is 44 mol%. The fluxes for L-lysine synthesis were calculated separately. The aspartate DH and dihydrodipicolinate DH carry a flux of 29.9 mol% (Fig. 3) and the diaminopimelate DH a flux of 14.3%, adding up to 74.1%. The transaminase flux is 46 mol% (29.9% aspartate amino transferase, plus 15.6% succinylaminotransferase). It follows that the sum of the NADPH-consuming fluxes is 194.9%, which is almost identical to the generating fluxes of 210.5%.

The flux balance for the heterologous mutant is shown in Fig. 5B. Here the glutamate dehydrogenase flux does not contribute to biosynthetic purposes due to the NAD-dependent dehydrogenase of *P. asaccharolyticus*. The NADPH flux of dehydrogenases required for biosynthetic purposes is comparable (51.6%), whereas the dehydrogenases operating

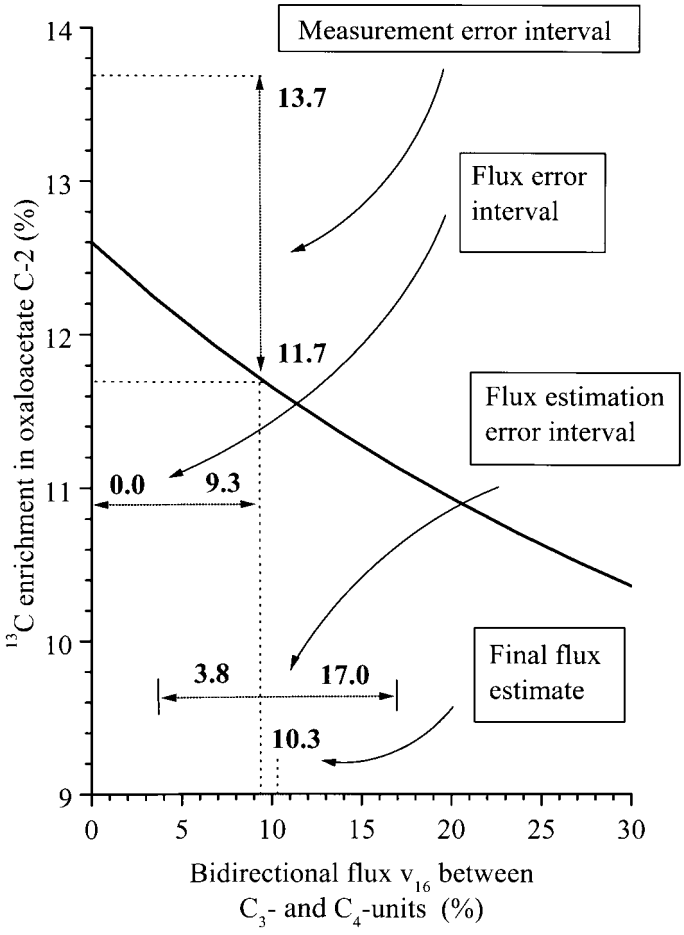


**FIG. 6.** Degree of $^{13}$C enrichment in C-2 of oxaloacetate as a function of the exchange flux $v_{16}^{\leftrightarrow}$ (exchange between C-4 and C-3 units). The dependency is given together with measured values, estimated values, and their statistical errors.

in L-lysine synthesis consume less NADPH, since in this particular experiment the total carbon flux toward L-lysine was reduced. However, importantly, as the response of the reduced NADPH demand due to the NAD-dependent glutamate DH, the generation of NADPH is drastically reduced. The total NADPH generating flux is 138.7 mol%. The consuming flux is calculated to be 95.3%, which gives an excess of 43.4%. This flux is exclusively accessible by the given isotope analysis and its relevance will be discussed below. About one fourth of the reduced NADPH demand in the heterologous mutant can be attributed to reduced demand for biomass synthesis and three fourths to that for L-lysine synthesis.

## DISCUSSION

Although it is often attempted, it is not possible to predict in a necessarily reductionist approach to describing the living cell how specific enzyme activities must be preset to result in the maximal output of the desired product. In contrast, the real benefit of such an approach is to be found elsewhere (Popper, 1974).This might be in our example the quantification of the intracellular flexibility or a deeper insight into the exchange fluxes.

We were able to identify such an exchange flux for a bacterium *in vivo* within the anaplerotic reactions (Marx *et al.*, 1996). The statistical analysis of this exchange flux in *C. glutamicum* shows that $v_{16}^{\leftrightarrow}$ (opposed carboxylating and decarboxylating reactions) is different in the two glutamate DH mutants analyzed. The 90% confidence interval for the heterologous mutant is 22.6–36.5% molar exchange flux, and the interval for the homologous mutant is 3.8–17.0% (Table 6). This difference results from the different levels of the $^{13}$C content for the oxaloacetate C-2 position (Tables 4 and 5). The enrichment in this position responds very sensitivly to the $v_{16}^{\leftrightarrow}$ exchange rate. The corresponding quantitative relation for the homologous mutant is shown in Fig. 6. The measured enrichment was $12.7 \pm 1.0$. Therefore, the molar exchange for the individually considered flux of $v_{16}^{\leftrightarrow}$ is 0–9.3% (relative to glucose uptake). Since the simulation considers all fluxes and exchanges, the estimated exchange between the C-3 units and the C-4 precursors as integrated in the total flux system is 10.3%, with a 90% confidence interval of 3.8–17.0%. The difference in the exchange flux between the two mutants had to be given as the sum of the individual fluxes interconverting the C-3 units and the C-4 units, since the partially identical educts and products do not yet permit any individual flux quantification. The situation is even more complex, since only recently has it become possible to clone the pyruvate carboxylase-encoding gene *pyc* (Peters-Wendisch *et al.*, 1998), which is therefore, in addition to phospho*enol*pyruvate carboxylase (*ppc*), the second reaction contributing to the net synthesis of oxaloacetate (Fig. 7). As mentioned, the partition of the carboxylating flux between the two carboxylase reactions identified is not yet known, nor is the physiological role of the backflux at this extensive set of enzymes around the anaplerotic reactions. In rats the backflux from pyruvate to oxaloacetate was estimated in isotopomer studies to be of approximately the same size as that from oxaloacetate to phospho*enol*pyruvate (Katz *et al.*, 1993). The backflux in *C. glutamicum* may indeed be of fundamental physiological significance (Fig. 7). Thus, an energy-consuming futile cycle without contributing to biosynthesis (Rognstadt, 1996) may be formulated via phospho*enol*pyruvate carboxykinase and pyruvate carboxylase. The inhibition of both enzymes by ADP corresponds to the idea that the ATP- and GTP-consuming cycle is reduced at a low energy charge. In glutamate production we found a very slight futile cycle flux between C-3 units and C-4 units of

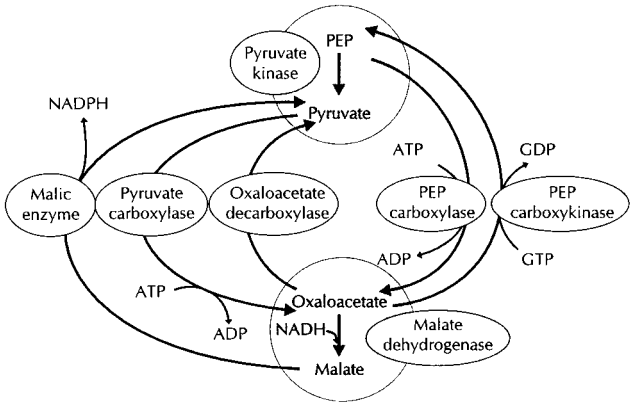


**FIG. 7.** Overview of the flux-carrying reactions at the anaplerotic node that could contribute to the reverse flux of 29.2% in the heterologous mutant, including a hypothetical transhydrogenase cycle and an energy-consuming cycle.

only 17.1% (Marx *et al.*, 1997). This could therefore be attributed to a low energy charge or increased conservation metabolism under the stress of biotin limitation. Another cycle which could be constructed consists of the malic enzyme and malate dehydrogenase resulting in the transfer of reducing equivalents from NAD to NADP. This cycle represents a transhydrogenase activity. There is contradictory information on *C. glutamicum* for a specific transhydrogenase (Cocaign-Bousquet and Lindley, 1996; Park *et al.*, 1997; Vallino 1991). In general, the sum of the carboxylating and decarboxylating reactions apparently serves as a fine tuning within the central metabolism to balance the fueling reactions with the catabolic reactions (Kornberg, 1966). Although the conversions between C-3 units and C-4 units seem to be important for the metabolic design of aromatic amino acid production in *E. coli* (Patnaik *et al.*, 1995), it is still unclear how they can be selectively used to increase amino acid overproduction. It is striking that with high C-4 unit formation the reverse flux is lowest in the homologous mutant of *C. glutamicum* (10.3%, see Fig. 3), as is the case under glutamate-producing conditions (Marx *et al.*, 1996). It is thus conceivable that the net conversion can be promoted not only by overexpression of, for example, pyruvate carboxylase, but also by reduction of the reverse fluxes.

As shown by the stoichiometry in Fig. 5, more NADPH is formed than is consumed. However, based on the 90% confidence interval, also the greater discrepany calculated for the heterologous mutant is still within the error range. Thus formation of an NADPH surplus cannot be quantified with certainty. Nevertheless, in all flux situations analyzed for *C. glutamicum* to date we have determined an excess of NADPH formation and never a deficit (Marx *et al.*, 1997; Sonntag *et al.*, 1995). Several additional reactions that are difficult to quantify might consume NADPH such as the system identified in *E. coli* detoxifying peroxide radicals (Luchi and Weiner, 1996), or an NAPDH-oxidizing activity which at least has been detected in extracts of *C. glutamicum* (Vallino, 1991). Also, a weak reaction of the *P. assacharolyticus* glutamate dehydrogenase using NADPH instead of NADH might be attributed to the greater discrepancy of the heterologous mutant, since the enzyme has a very low activity of 0.9% with NADPH as substrate.

In any case, the cell (Fig. 5) actually responded by reduced redox generation through our selective intervention of diminished demand for redox equivalents. There are several examples of cases where externally added electron mediators might affect the intracellular redox metabolism as inferred from an altered product spectrum (Neijssel 1977; Kwong and Rao, 1992). An internal alteration of the NADPH balance was obtained in yeast by the synthesis of an NADPH-dependent xylose reductase, which led to altered by-product formation (Meinander *et al.*, 1996). Our quantitative data show that for the directly altered NADPH demand the NADPH generation is reduced by about one-third. It thus follows that *C. glutamicum* is enormously flexible not only with respect to the carbon fluxes in the central metabolism (Marx *et al.*, 1997) but also with respect to the redox fluxes. This could be a reason for the particular suitability of this bacterium for metabolite overproduction. Since our data show that the cell adjusts the fluxes to the reduced NADPH demand and does not use a potentially available increased NADPH supply to increase lysine production, we regard this as an indication that lysine production is not essentially NADPH-limited. However, this question must be addressed in further studies by direct intracellular quantification of the involved metabolites.

In total, we have now generated a unique set of five different flux situations of isogenic strains specifying the response of the metabolism to an altered carbon or reducing power flux. Acting only on one enzyme activity, for instance, a kinase (Marx *et al.*, 1997) or a dehydrogenase (this work), results in an extreme range of fluxes in the central metabolism. The oxidative PPP carbon flux varies from 25 to 76%. As a general trend, it can be seen that at a high NADPH demand a high PPP flux results. Furthermore, there is an inverse relation of the PPP flux to the TCC flux. A global picture of flux regulation in *C. glutamicum* can thus be derived. The TCC flux is first adjusted according to the carbon requirements. The isocitrate dehydrogenase activity necessarily linked to the latter provides a basal level of NADPH flux. In extreme cases this is manifest in glutamate production, where a high input into the TCC is present due to the high α-ketoglutarate requirement. However, there is still high cycling activity due to the α-ketoglutarate DH activity present, which was originally thought to be absent in *C. glutamicum* (Kinoshita, 1985). This activity

serves to provide sufficient NADH for ATP generation. Whereas in the TCC cycle the fluxes are adjusted to the specific carbon and NADH demand, the PPP flux is adjusted according to the NADPH demand not fulfilled by the TCC. With high TCC flux (glutamate production) the PPP flux is thus reduced, whereas at low TCC flux (lysine production) the PPP flux is high to adjust the NADPH balance. The specific regulators controlling the entry into the PPP are the glucose-6-P DH and 6-P-gluconate DH, both controlled in their catalytic acitivity by the NADPH concentration via allosteric mechanisms (Sugimoto and Shiio, 1987). Due to the flexibility of the central metabolism and its design to provide precursors as well as NADPH and NADH, it appears that the major targets to be altered to obtain maximal productivities are the biosynthesis pathways themselves, together with the export of the metabolite to be produced. What might limit maximal product formation beyond these reactions cannot be predicted by mechanistic flux studies, but relates to questions concerning the cell in its entirety, for instance, the tolerance of the cell toward physical features of the product, or how controlled reduction of precursor use for biomass formation can be obtained.

## ACKNOWLEDGMENTS

We thank E. Börmann, K. Krumbach, and S. Petrovic for help with constructions and analyses, M. Tesch for sharing results prior to publication, and W. Wiechert (University of Siegen), D. Molenaar (University of Düsseldorf), and V. Wendisch (University of California, Berkeley) for discussions.

## REFERENCES

Berry, A. (1996). Improving production of aromatic compounds in *Escherichia coli* by metabolic engineering. *TIBTECH* **14**, 250–256.

Börmann, E., Eikmanns, B. J., and Sahm, H. (1992). Molecular analysis of the *Corynebacterium glutamicum gdh* gene encoding glutamate dehydrogenase. *Mol. Microbiol.* **6**, 317–326.

Cocaign-Bousquet, M., Guyonvarch, A., and Lindley, N. D. (1996). Growth-rate dependent modulation of carbon flux through central metabolism and the kinetic consequences for glucose-limited chemostat cultures of *Corynebacterium glutamicum*. *Appl. Environ. Microbiol.* **62**, 429–436.

Eggeling, L., DeGraaf, A. A., and Sahm, H. (1996). Quantifying and directing metabolite flux: Application to amino acid overproduction. *Adv. Biochem. Eng.* **54**, 2–30.

Eggeling, L., Oberle, S., and Sahm, H. (1997). Improved L-lysine yield with *Corynebacterium glutamicum*: Use of *dapA* resulting in increased flux combined with growth limitation. *Appl. Microbiol. Biotechnol.* **49**, 24–30.

Eggeling, L., Morbach, S., and Sahm, H. (1997). The fruits of molecular physiology: Engineering the L-isoleucine biosynthesis pathway in *Corynebacterium glutamicum*. *J. Biotechnol.* **56**, 167–182.

Eggeling, L., and Sahm, H. (1998). Amino acid production: Principles of metabolic engineering. *In* "Metabolic Engineering" (Y. S. Sang and E. T. Papoutsakis, Eds.), Biotechnology Intelligence Unit, R. G. Landes.

Eikmanns, B., Kleinertz, E., Liebl, W., and Sahm, H. (1991). A family of *Corynebacterium glutamicum*/*Escherichia coli* shuttle vectors for gene cloning, controlled gene expression, and promoter probing. *Gene* **102**, 93–98.

Flores, N., Xiao, J., Berry, A., Bolivar, F., and Valle, F. (1996). Pathway engineering for the production of aromatic compounds in *Escherichia coli*. *Nature Biotechnol.* **14**, 620–623.

Iuchi, S., and Weiner, L. (1996). Cellular and molecular physiology of *Escherichia coli* in the adaption to aerobic environments. *J. Biochem.* **120**, 1055–1063.

Katz, J., Wals, P., and Lee, W. P. (1993). Isotopomer studies of gluconeogenesis and the Krebs cycle with $^{13}$C-labeled lactate. *J. Biol. Chem.* **268**, 25509–25521.

Kinoshita, S. (1985). Glutamic acid bacteria. *In* "Biology of Industrial Microorganisms" (A. L. Demain and N. A. Solomon, Eds.), pp. 115–142, Benjamin/Cummings, Redwood City, CA.

Kornberg, H. L. (1966). Anaplerotic sequences and their role in metabolism. *In* "Essays in Biochemistry" (P. N. Campbell and G. D. Grevile, Eds), Vol II, pp. 1–31, Academic Press, New York.

Kwong, S. C. W., and Rao, G. (1992). Effect of reducing agents in an aerobic amino acid fermentation. *Biotechnol. Bioeng.* **40**, 851–857.

Liebl, W., Bayerl, A., Stillner, U., and Schleifer, K. H. (1989). High efficiency electroporation of intact *Corynebacterium glutamicum* cells *FEMS Microbiol. Lett.* **65**, 299–304.

Marx, A., de Graaf, A. A., Wiechert, W., Eggeling, L., and Sahm, H. (1996). Determination of the fluxes in the central metabolism of *Corynebacterium glutamicum* by NMR spectroscopy combined with metabolite balancing. *Biotechnol. Bioeng.* **49**, 111–129.

Marx, A., Striegel, K., de Graaf, A. A., Sahm, H., and Eggeling, L. (1997). Response of the central metabolism of *Corynebacterium glutamicum* to different flux burdens. *Biotechnol. Bioeng.* **56**, 168–180.

Meinander, N., Zacchi, G., and Hah-Hägerdal, B. (1996). A heterologous reductase affects the redox balance of recombinant *Saccharomyces cerevisiae*. *Microbiology* **142**, 165–172.

Mori, M., and Shiio, I. (1985). Purification and some properties of phosphoenolpyruvate carboxylase from *Brevibacterium flavum* and its aspartate-overproducing mutant. *J. Biochem. Tokyo* **97**, 1119–1128.

Mori, M., and Shiio, I. (1985). Synergistic inhibition of phosphoenolpyruvate carboxylase by aspartate and 2–oxoglutarate in *Brevibacterium flavum*. *J. Biochem. Tokyo* **98**, 1621–1630.

Neese, R. A., and Hellerstein, M. K. (1995). Calculations for gluconeogenesis by mass isotopomer distribution analysis. *J. Biol. Chem.* **276**, 14464–14466.

Neijssel, O. M. (1977). The effect of 2,4–dinitrophenol on the growth of *Klebsiella aerogenes* NCTC 418 in aerobic chemostat cultures. *FEMS Lett.* **1**, 47–50.

Oshima, K., Tanaka, K., and Kinoshita, S. (1964). Studies on L-glutamic acid fermentation. XI. Purification and properties of L-glutamic dehydrogenase from *Micrococcus glutamicus*. *Agric. Biol. Chem. Tokyo* **28**, 714–722.

Park, S. M., Sinskey, A. J., and Stephanopoulos, G. (1997). Metabolic and physiological studies of *Corynebacterium glutamicum* mutants. *Biotechnol. Bioeng.* **55**, 864–879.

Patnaik, R., Spitzer, R. G., and Liao, J. C. (1995). Pathway engineering for production of aromatics in *Escherichia coli*: Confirmation of stoichiometric analysis by independent modulation of AroG, TktA, and Pps activities. *Biotechnol. Bioeng.* **46**, 361–370.

Peters-Wendisch, P., Kreutzer, C., Kalinowski, J., Pátek, M., Sahm, H., and Eikmanns, B. J. (1998). Pyruvate carboxylase from *Corynebacterium glutamicum*: Characterization, expression and inactivation of the *pyc* gene. *Microbiol. UK* **143**, 1095–1103.

Peters-Wendisch, P. G., Wendisch, V. F., Paul, S., Eikmanns, B. J., and Sahm, H. (1997). Pyruvate carboxylase as an anaplerotic enzyme in *Corynebacterium glutamicum*. *Microbiol. UK* **143**, 1095–1103.

Popper, K. (1974). "Studies on the Philosophy of Biology." (F. J. Ayda and T. Dobzhansky, Eds.), pp. 259–283, MacMillan, London.

Rognstad, R. (1996). Futile cycling in carbohydrate metabolism. I. Background and current controversies on pyruvate cycling. *Biochem. Arch.* **12**, 71–83.

Sauer, U., Hatzimanikatis, V., Hohmann, H., Manneberg, M., van Loon, A., and Bailey (1996). Physiology and metabolic fluxes of wild-type and riboflavin-producing *Bacillus subtilis*. *Appl. Environ. Microbiol.* **62**, 3687–3696.

Schäfer, A., Kalinowski, J., Simon, R., Seep-Feldhaus, A., and Pühler, A. (1990). High-frequency conjugal plasmid transfer from gram-negative *Escherichia coli* to various gram-positive coryneform bacteria. *J. Bacteriol.* **172**, 1663–1666.

Schäfer, A., Tauch, A., Jäger, W., Kalinoski, J., Thierbach, G., and Pühler, A. (1994). Small mobilizable multi-purpose cloning vectors derived from the *Escherichia coli* plasmids pK18 and pK19: Selection of defined deletions in the chromosome of *Corynebacterium glutamicum*. *Gene* **145**, 69–73.

Schrumpf, B., Eggeling, L., and Sahm, H. (1992). Isolation and prominent characteristics of an L-lysine hyperproducing strain of *Corynebacterium glutamicum*. *Appl. Microbiol. Biotechnol.* **37**, 566–571.

Schwarzer, A., and Pühler, A. (1990). Genetic manipulation of the amino acid-producing *Corynebacterium glutamicum* strain ATCC 13032 by gene disruption and gene replacement. *Bio/Technology* **9**, 84–87.

Simon, R., Priefer, U., and Pühler, A. (1983). A broad host range mobilization system for in vivo genetic engineering: Transposon mutagenesis in gram negative bacteria. *Bio/Technology* **1**, 784–791.

Snedecor, B., Chu, H., and Chen, E. (1991). Selection, expression, and nucleotide sequencing of the glutamate dehydrogenase gene of *Peptostreptococcus asaccharolyticus*. *J. Bacteriol.* **173**, 6162–6167.

Sonntag, K., Schwinde, J., de Graaf, A. A., Marx, A., Eikmanns, B. J., Wiechert, W., and Sahm, H. (1995). 13–C NMR studies of the fluxes in the central metabolism of *Corynebacterium glutamicum* during growth and overproduction of amino acids in batch cultures. *Appl. Microbiol. Biotechnol.* **44**, 489–495.

Sugimoto, S., and Shiio, I. (1987). Regulation of glucose-6–phosphate dehydrogenase in *Brevibacterium flavum*. *Agric. Biol. Chem. Tokyo* **51**, 101–108.

Vallino, J. J. (1991). "Identification of Branch-Point Restrictions in Microbial Metabolism Through Metabolic flux Analysis and Local Network Perturbations." Ph.D. thesis, Massachusetts Insitute of Technology, Boston.

Vallino, J. J., and Stephanopoulos, G. (1993). Metabolic flux distributions in *Corynebacterium glutamicum* during growth and lysine overproduction. *Biotechnol. Bioeng.* **41**, 633–646.

Vrljic, M., Sahm, H., and Eggeling, L. (1996). A new type of transporter with a new type of cellular function: L-Lysine export in *Corynebacterium glutamicum*. *Mol. Microbiol.* **22**, 815–826.

Weisbrod, R. E., and Meister, A. (1973). Studies on glutamine synthetase from *Escherichia coli*. *J. Biol. Chem.* **248**, 3997–4002.

Wendisch, V. F., de Graaf, A. A., and Sahm, H. (1997). Accurate determination of $^{13}C$ enrichments in nonprotonated carbon atoms of isotopically enriched amino acids by $^{1}H$ nuclear magnetic resonance. *Anal. Biochem.* **245**, 196–202.

Wiechert, W., Siefke, C., de Graaf, A. A., and Marx, A. (1997). Bidirectional reaction steps in metabolic engineering. II. Flux estimation and statistical analysis. *Biotechnol. Bioeng.* **55**, 118–135.

Wiechert, W., and de Graaf, A. A. (1997). Bidirectional reaction steps in metabolic engineering; Modeling and simulation of carbon isotope labeling experiments. *Biotechnal Bioeng.* **55**, 101–117.